Rev Osteoporos Metab Miner. 2020;12(2):45-52

Can 3D measurements obtained by lumbar DXA predict fractures in the dorsal vertebrae?

DOI: http://dx.doi.org/10.4321/S1889-836X2020000200003

López Picazo M[1,2], Humbert L[1], Di Gregorio S[3], González Ballester MA[2,4], Del Río Barquero LM[3]
1 Musculoskeletal Unit. Galgo Medical. Barcelona (Spain)
2 BCN Medtech (Barcelona Center for New Medical Technologies). Pompeu Fabra University. Barcelona (Spain)
3 CETIR Grupo Médico. Barcelona (Spain)
4 ICREA (Catalan Institution for Research and Advanced Studies). Barcelona (Spain)

Date of receipt: 28/06/2019 - Date of acceptance: 27/02/2020

Work awarded with a scholarship to attend the 40th ASBMR Congress (Montreal, 2018)

Summary

Objective: To assess the relation between three-dimensional (3D) measurements obtained by lumbar dual energy X-ray absorptiometry (DXA) and osteoporotic fractures in dorsal vertebrae.

Material and methods: We analysed retrospectively 32 postmenopausal women, allocated to two groups: 16 women in the experimental group, who presented incident fractures of the dorsal vertebrae, and 16 women in the control group, who did not show any type of fracture. Measurements of the (aBMD) of vertebrae L1 through L4 were taken at the initial visit (i.e., prior to the fracture event) by lumbar dual-energy x-ray absorptiometries (DXA). 3D measurements obtained by DXA were evaluated using 3D modelling software (3D-SHAPER). Volumetric bone mineral density (vBMD) was calculated in the trabecular, cortical and integral bone. Cortical thickness and cortical surface BMD (sBMD) were also measured. Differences in measurements derived from the DXA between the experimental and control groups were assessed using an unpaired Student t-test. The odds ratio (OR) and the area under the receiver operating characteristic curve (AUC) were also determined.

Results: In the present age-adjusted case-control study, no significant differences were found between the experimental and control groups in terms of weight (ρ=0.44), height (ρ=0.25) and aBMD (ρ=0.11). However, significant differences (ρ<0.05) were found in the integral and trabecular vBMD and in the cortical sBMD. Trabecular vBMD in the vertebral body was the measure that best discriminated between both groups, with an AUC of 0.733, compared to 0.682 of the aBMD.

Conclusion: This study shows the ability of 3D models resultant from lumbar DXAs to discern between subjects with incident fractures in the dorsal vertebrae and control subjects. It is necessary to analyse larger cohorts to establish if these measurements could improve the prediction of fracture risk in clinical practice.

Key words: 3D modelling, fracture risk, osteoporosis, trabecular, cortical, vertebral fracture, volumetric bone mineral density, superficial bone mineral density.

Introduction

Every year 8.9 million osteoporosis-related fractures occur worldwide, representing one fracture every 3 seconds[1], with vertebral being the most common osteoporotic fractures[2].

Dual-energy X-ray absorptiometry (DXA) is the standard test for diagnosing osteoporosis and evaluating fracture risk[3,4], as it is a low-radiation, inexpensive technique. The DXA provides two-dimensional (2D) images that measure the bone mineral density of the area (aBMD) projected along the anteroposterior (AP) direction. Various studies show that a low aBMD value, measured in AP DXA explorations, is among the highest fracture risks[3-5]. The decrease of the aBMD standard deviation leads to an increase from 1.5 up to 3.0 times the risk of fracture, depending on its location and its measurement's location[5]. Nevertheless, a low BMD value is not enough to explain every fracture. Recent studies suggest that the risk of fracture is high when the BMD value is low, but this does not mean that fracture risk is negligible when the BMD value is normal[3-8].

Correspondence: Mirella López Picazo (mirella.lopez.picazo@gmail.com)

Most osteoporosis-related vertebral fractures are located in the vertebral body[9]. In AP DXA images of the spinal column, the vertebral body overlaps the posterior vertebral elements, so the BMD in the vertebral body cannot be estimated separately. On the other hand, the risk of fracture depends on the architecture of the trabecular bone and the thickness of the cortical bone[10]. However, the trabecular and cortical bone compartments are difficult to assess separately on AP DXA scans.

As an alternative to the DXA, quantitative computed tomography (QCT) provides a three-dimensional (3D) analysis of the bone structures. In QCT imaging, the volumetric BMD (vBMD) can be measured in the vertebral body alone, separate from the posterior vertebral elements, and even trabecular and cortical structures can be evaluated in isolation[3,11,12]. Previous studies have appraised the association between vBMD derived from QCT and vertebral fractures[8,13-17]. Finite element models based on QCT have also been analysed to know the mechanical properties of the vertebrae and to predict the risk of vertebral fracture[17-20]. However, QCT scans compared to DXA scans involve exposure to a higher dose of radiation, as well as a higher cost. As a consequence, QCT is rarely used in clinical practice for fracture risk assessment.

In order to overcome the limitations of the DXA and QCT scans, various researches suggest the use of 3D modelling methods to determine the shape and distribution of bone density considering a limited number of DXA scans[21-25]. These studies use a three-dimensional statistical model of the bone shape and density which is recorded in DXA examinations to obtain a personalized 3D model of such bone (QCT type). The precision of these methods[21-25] has been evaluated by comparing 3D models and measurements obtained via DXA and QCT. However, as far as we know, no study has been conducted on the association of measurements provided by DXA-based 3D modelling techniques and vertebral fractures.

On another note, AP DXA usually includes only the lumbar region (L1 to L4), since the rib cage overlaps in the projection, avoiding the use of DXA to determine the aBMD in the thoracic spine. Despite this, various studies indicate that the greatest number of vertebral fractures related to osteoporosis occur at the thoracoabdominal junction (T12-L1)[15,26]. Although the reason for this higher prevalence is unknown, it has been suggested that thoracic kyphosis and rib cage stiffness predispose this area to fracture as the vertebral load is higher at this location. Even though measurements made at the same fracture location show a greater power of discrimination, Budoff et al.[27] found a high correlation between trabecular vBMD in the lumbar vertebrae and trabecular vBMD in the dorsal vertebrae.

The objective of this study was to assess the ability of 3D measurements derived from the DXA to distinguish subjects with incident fractures of the dorsal vertebrae from control subjects. To do this, a retrospective case-control study was carried out, which included postmenopausal Caucasian females who experienced a fracture event in the dorsal vertebrae (cases) and control females of the same age without any type of fracture. For each subject, 3D measurements derived from lumbar DXA were obtained at the initial baseline visit (which took place at least one year prior to the vertebral fracture event for subjects in the experimental group) using lumbar DXA AP scans and a DXA-based 3D modelling technique[25].

Materials and methods

Study population

We analyzed in retrospect a database compiled at CETIR Grup Mèdic (Barcelona, Spain). The database is made up of postmenopausal Caucasian women over the age of 40 who have already had an initial baseline and follow-up visit, both conducted between the years 2000 and 2010. Subjects in the database were stratified into two groups: patients with incident fractures in the dorsal vertebrae related to osteoporosis (experimental group) and subjects without any type of fracture (control group). The inclusion criteria in the experimental group were: absence of prevalent osteoporotic fractures, incident osteoporotic fracture of the dorsal vertebrae during the follow-up period (between one and ten years from the initial baseline visit), and absence of non-vertebral osteoporotic fractures during the follow-up period. The inclusion criteria in the control group were: absence of any type of osteoporotic fracture at the time of the initial baseline visit and for at least seven years following it. The individuals in both groups were excluded if they had undergone spinal surgery or had any bone disease other than osteoporosis, such as severe osteoarthritis, severe scoliosis, spondylitis, spinal infection, or abnormal bone growth. Each subject in the experimental group was age-matched (± 5 years) with a subject in the control group (1:1). Clinical parameters such as age, weight, height, and body mass index (BMI) were collected from each subject at the initial baseline visit. The database used in this study is part of a previous study in which the relation between 3D measurements derived from lumbar DXA and different types of vertebral fractures was evaluated[28].

Vertebral fractures were confirmed by a radiologist, who used the evaluation of vertebral fractures according to the Genant semi-quantitative classification criteria[9]. The absence of fracture was determined by reviewing the clinical history of the subjects, analyzing the AP DXA examinations at the baseline and follow-up visits, and ruling out the subjects whose height decreased by 2 cm or more between the reference visit and the follow-up visit. The presence (experimental group) or absence (control group) of fractures in the dorsal vertebrae could not be confirmed by morphometry for all the subjects, so the study is limited to clinical fractures.

This study was conducted as stipulated by the latest version of the Declaration of Helsinki. The Scientific Committee of the CETIR Grup Mèdic gave its ethical approval for the use of retrospective clinical data and the measurement results within the scope of this study. Anonymity of each subject was ensured and maintained by using numerical codes for all records.

Medical images and 2D measurements derived from DXA

All the subjects included in the study went through a lumbar AP DXA examination at the baseline visit. DXA scans were carried out with a Prodigy densitometer (GE Healthcare, Madison, Wisconsin, USA) and analysed with the enCORE software (v14.10, GE Healthcare, Madison, Wisconsin, USA). DXA scans and analyses were performed by a radiologist at CETIR Grup Mèdic in accordance with the manufacturer's recommendations. 2D measurements derived from DXA, such as aBMD (in g/cm^2), bone mineral content (BMC, in g), and area (in cm^2), were measured for L1 to L4 vertebrae in the AP DXA examinations. The T-score was evaluated using the GE-Lunar reference curves for Spain.

3D measurements derived from the DXA

3D measurements derived from the DXA in the L1-L4 segment were obtained with 3D-SHAPER software (Galgo Medical, Barcelona, Spain) and AP DXA scans taken at the initial baseline visit (before fracture). 3D-SHAPER calculates a custom 3D model of the lumbar spine shape and density from a single AP DXA image, as described in López Picazo et al.[25] and is briefly summarized next. First, the custom 3D estimate is obtained by registering and fitting a statistical model of shape and density in the AP DXA image. The statistical model is previously generated using a training database of QCT scans of Caucasian men and women. The cortical bone of the vertebral body is then segmented using an algorithm based on intensity models[25,29]. This algorithm calculates the density profile along the normal vector at each node of the 3D surface mesh and adjusts it to a function defined by the thickness and cortical density, the location of the cortical cortex, the density of the surrounding tissues and the blur of the image. Finally, 3D measurements derived from the DXA are taken in different vertebral regions and bone compartments. The vBMD (in mg/cm^3), the BMC (in g) and the volume (in cm^3) were measured in the integral bone of the total vertebra and the vertebral body. These same measurements were also obtained for the trabecular and cortical compartments in the vertebral body. The average cortical thickness (Cort. Th., in mm) and the cortical surface bone mineral density (cortical sBMD, in mg/cm^2) were measured in the vertebral body. Cortical sBMD is the amount of cortical bone per unit area integrated along the normal vector at each node of the vertebral body surface mesh. It was calculated as the multiplication of the cortical vBMD (in mg/cm^3) and the Cort. Th. (in cm).

Statistical analysis

Descriptive statistics, including mean and standard deviation, were used to analyze both the experimental and control groups at the initial baseline visit. The differences between the groups were assessed using the unpaired Student t-test, after verifying the normality of the data. A value of $p<0.05$ was considered statistically significant. Invariant logistic regressions were used to investigate possible correspondence between independent variables (weight, height, BMI, 2D and 3D measurements obtained by DXA) and the state of the fracture. The ability of DXA-derived measurements to discriminate between subjects with fractures and control subjects was assessed using the area under the receiver operating characteristic curve (AUC). The odd ratio (OR) was calculated with 95% confidence intervals (CI) to estimate the odds of a vertebral fracture occurring at any change of one standard deviation in measurements obtained by the DXA. The mean of the 3D shape and the density to visualize the differences in the distribution of vBMD were calculated for each group. Cuts in the median plane of the vertebral body were used to display the anatomical distribution of the differences in vBMD. The distribution of cortical sBMD was also calculated for each group. The differences in cortical sBMD distribution were shown in one instance of the average shape. Statistical analyses were carried out using Matlab Academic (version R2015b, MathWorks, Inc., Natick, Massachusetts, USA).

Results

Characteristics of the subjects

32 postmenopausal Caucasian women were included in this study: 16 patients with at least one incident osteoporotic fracture of the dorsal vertebrae (experimental group) and 16 subjects of the same age without any type of fracture (control group). The fractured group consisted of 11 subjects with a single fractured dorsal vertebra and 5 subjects with multiple vertebral fractures. A total of 25 incident vertebral fractures were found in the patients in the fracture group: two T4, two T7, one T8, one T9, three T10, one T11, nine T12, five L1 and one L2. It is unknown whether the vertebral fractures presented wedge, biconcave or crush deformities.

Patients in the experimental group had a vertebral fracture event at an average (± standard deviation) of 3.2±2.4 years from the initial baseline visit. The absence of osteoporotic fracture events was ensured for the controls during an average period of 8.4±1.0 years. No significant differences ($\rho \geq 0.05$) were observed between the experimental and control groups in terms of age, weight, height and BMI (Table 1).

2D measurements derived from DXA

In line with WHO classification criteria, 94% of the patients in both groups presented a low aBMD (T-score for L-L4 <-1). The experimental group included 12 women with osteoporosis, 3 with low bone mass and 1 with normal bone mass; while the control group included 5 women with osteoporosis, 10 with low bone mass and 1 with normal bone mass.

The mean aBMD in the L1-L4 segment of the subjects in the experimental group was 8.1% lower compared to those in the control group, although not significant ($p=0.11$; table 2). There were also no significant differences in BMC and AREA ($p>0.05$). The aBMD differentiated between the experimental group and the control group with an AUC=0.662. Each decrease in one standard deviation in the aBMD was associated with an almost two-fold increase in the probability of presenting an osteoporotic fracture in the dorsal vertebrae (OR=1.862; 95% CI: 0.862-4.022).

Table 1. Characteristics of the subjects at the initial baseline visit

	Controls	Fractured	p*
Number	16	16	
Age (years)	63.9 ± 7.7 [50.0 - 74.0]	64.9 ± 8.4 [48.8 - 75.7]	0.738
Weight (kg)	61.7 ± 10.1 [46.0 - 85.0]	64.2 ± 8.2 [54.0 - 83.0]	0.444
Height (cm)	154.0 ± 4.7 [143.0 - 161.0]	156.0 ± 5.1 [148.0 - 169.5]	0.251
BMI (kg/m^2)	26.0 ± 3.6 [21.0 - 32.8]	26.4 ± 2.9 [22.0 - 30.8]	0.733

Results expressed as mean ± standard deviation [minimum - maximum]; *: p values of the unpaired Student t-test; BMI: body mass index.

3D measurements derived from the DXA

The integral vBMD in the total vertebra in the experimental group was 10.2% lower than in the control group (p<0.05; table 2). In the vertebral body, the differences in vBMD were more pronounced in the trabecular bone (-16.2%, p<0.01) than in the integral bone (-12.8%, p<0.01). Cortical vBMD in the vertebral body was 2.3% lower in the experimental group, as well as non-significant (p=0.477). The cortical vBMD in the vertebral body in the experimental group was 10.0% lower than in the control group (p=0.018). The anatomical distribution of the mean differences between the trabecular vBMD in the vertebral body of the subjects included in the fractured and control groups is shown in figure 1. In it, we can see how the differences in the trabecular vBMD are more pronounced near the end plates of the vertebral body.

The trabecular vBMD in the vertebral body was related to higher values of AUC (0.801) and OR (5.060; 95% CI: 1.406-18.208), compared to other measurements derived from DXA (Table 2). Slightly lower values were found for the integral vBMD in the vertebral body (AUC=0.793 and OR=4.557; 95% CI: 1.411-14.718). The AUC map associated with the trabecular vBMD values calculated at each voxel of the volumetric images of the subjects included in the experimental and control groups is shown in figure 2. Only the AUC of the 90th percentile (AUC>0.720) are represented. A maximum AUC value of 0.815 was reached. Trabecular vBMD measurements show a higher AUC value near the end plates.

Cortical sBMD in the vertebral body was connected to higher values of AUC (0.734) and OR (2.649; 95% CI: 1.111-6.313), compared to other measurements made on cortical bone (Table 2). The anatomical distribution of the mean differences in cortical sBMD between the subjects included in the experimental and control

Table 2. Measurements derived from the DXA of the initial baseline visit in both groups, differences between groups, AUC and OR

L1-L4	Controls	Fractured	Differences	p*	AUC	OR [IC 95%]
2D measurements derive from DXA						
aBMD	0.931 ± 0.126	0.856 ± 0.133	-0.076 (-8.1%)	0.110	0.662	1.862 [0.862 - 4.022][a]
BMC	46.6 ± 7.8	44.4 ± 9.6	-2.7 (-5.8%)	0.392	0.613	1.382 [0.672 - 2.841][a]
Area	50.0 ± 3.9	51.1 ± 6.2	1.2 (2.4%)	0.523	0.488	0.785 [0.382 - 1.614][b]
3D measurements derived from the DXA						
Integral bone, total vertebra						
Int. vBMD	256.2 ± 36.6	230.0 ± 34.0	-26.2 (-10.2%)	**0.044**	0.691	2.296 [0.974 - 5.413][a]
Int. BMC	40.5 ± 6.9	38.1 ± 8.4	-2.4 (-6.0%)	0.379	0.602	1.394 [0.677 - 2.868][a]
Int. volume	157.9 ± 14.1	165.2 ± 23.7	7.3 (4.6%)	0.300	0.574	0.670 [0.317 - 1.417][b]
Integral bone, vertebral body						
Int. vBMD	207.6 ± 24.1	181.0 ± 20.5	-26.6 (-12.8%)	**0.002**	0.793	4.557 [1.411 - 14.718][a]
Int. BMC	21.3 ± 3.1	19.2 ± 3.9	-2.1 (-9.7%)	0.109	0.652	1.865 [0.863 - 4.029][a]
Int. volume	102.6 ± 9.3	105.8 ± 15.5	3.2 (3.1%)	0.484	0.531	0.766 [0.371 - 1.583][b]
Trabecular bone, vertebral body						
Trab. DMOv	134.5 ± 21.2	112.7 ± 16.3	-21.8 (-16.2%)	**0.003**	0.801	5.060 [1.406 - 18.208][a]
Trab. BMC	12.0 ± 2.0	10.5 ± 2.0	-1.5 (-12.7%)	**0.038**	0.688	2.338 [0.996 - 5.486][a]
Trab. volume	89.4 ± 8.7	93.3 ± 13.8	3.8 (4.3%)	0.357	0.563	0.702 [0.334 - 1.473][b]
Cortical bone, vertebral body						
Cort. vBMD	704.3 ± 47.9	687.9 ± 77.2	-16.3 (-2.3%)	0.477	0.543	1.307 [0.639 - 2.673][a]
Cort. BMC	9.3 ± 1.4	8.7 ± 2.2	-0.6 (6%)	0.401	0.570	1.373 [0.668 - 2.823][a]
Cort. volume	13.2 ± 1.3	12.5 ± 1.9	-0.6 (-4.7%)	0.294	0.621	1.492 [0.716 - 3.110][a]
Cort. Th.	0.66 ± 0.06	0.62 ± 0.05	-0.05 (-7.1%)	**0.017**	0.734	2.659 [1.115 - 6.342][a]
Cort. BMDs	52.2 ± 6.5	47.0 ± 5.1	-5.2 (-10.0%)	**0.018**	0.734	2.649 [1.111 - 6.313][a]
Cortical bone, regions of the vertebral body						
Cort. BMDs (Higher)	58.7 ± 8.0	52.5 ± 5.8	-6.3 (-10.7%)	**0.017**	0.730	2.722 [1.115 - 6.644]
Cort. BMDs (Lower)	56.9 ± 6.8	51.5 ± 5.7	-5.3 (-9.4%)	**0.023**	0.754	2.793 [1.060 - 7.358]
Cort. BMDs (Previous)	41.1 ± 7.4	35.9 ± 5.9	-5.3 (-12.8%)	**0.035**	0.699	2.363 [1.020 - 5.477]
Cort. BMDs (Later)	54.1 ± 8.8	50.1 ± 8.8	-4.0 (-7.4%)	0.209	0.637	1.629 [0.762 - 3.480]

Measurements of the experimental and control groups are expressed as mean ± standard deviation. Differences between groups are expressed as mean (percentage). *: p values of the unpaired Student t-test; p values <0.05 are shown in bold; [a]: probability ratio corresponding to a standard deviation of decrease in the measure; [b]: probability ratio corresponding to a standard deviation of increase in the measurement; AUC: area below the receiver operating characteristic curve; OR: odds ratio; CI: confidence interval; Int.: integral; Trab.: trabecular; Cort.: cortical; aBMD: areal bone mineral density (g/cm^2); BMC: bone mineral content (g); area (cm^2); vBMD: volumetric bone mineral density (mg/cm^3); volume (cm^3); Cort. Th .: cortical thickness (mm); BMDs: surface bone mineral density (mg/cm^2); Int.: integral bone; Trab.: trabecular bone; Cort.: cortical bone; Total: total vertebra; Body: vertebral body.

groups, is shown in figure 3 (top). More pronounced differences (magenta-coloured) were found in the end plates of the L1, L2 and L4 vertebrae. The cortical sBMD in the lower end plate was the measure of sBMD with the highest AUC (0.754) and OR (2.793; 95% CI: 1.060-7.358) values. Figure 3 (bottom) shows the AUC value calculated using cortical sBMD at each vertex of the vertebral body surface. AUC values of the 90th percentile (i.e. in the range of 0.777-0.836) are circled in red and were found mainly on the end plates.

Discussion

In the present study, the ability of 3D measurements derived from lumbar DXA, to discriminate between postmenopausal women with and without osteoporotic fractures in the dorsal vertebrae, was evaluated. 3D measurements derived from the DXA were performed at the initial baseline visit (at least one year before the vertebral fracture event), using standard DXA scans and a 3D modelling technique[25].

Age, gender, and BMI are independent risk factors for osteoporosis-related fractures[3,4]. In this study, a database of postmenopausal females paired by age was used to eliminate the possible effect of age and gender on the results. Although inclusion criteria related to height or weight were not used to recruit subjects, no significant differences were found between the groups in terms of height, weight, and BMI at the initial baseline visit.

No significant differences were observed in the aBMD (-8.1%, p=0.110), but in the integral vBMD (-10.2%, p=0.044). On the other hand, higher ORs were found for the vBMD measurements obtained via DXA in the verte-

Figure 1. Anatomic distribution of the mean differences in trabecular vBMD, between the subjects included in the experimental group and those in the control group. The differences are shown in the mid-coronal plane (centre) and the median lateral plane (right) of the vertebral body. The image on the left shows the plans that were used. The red-yellow areas indicate the regions where the difference in trabecular vBMD between the subjects with vertebral fracture and the control subjects is on average lower (in blue-green areas this difference is higher). Non-significant changes (unpaired Student t-test) were marked in black. The pink outline indicates the periosteal surface of the vertebral body

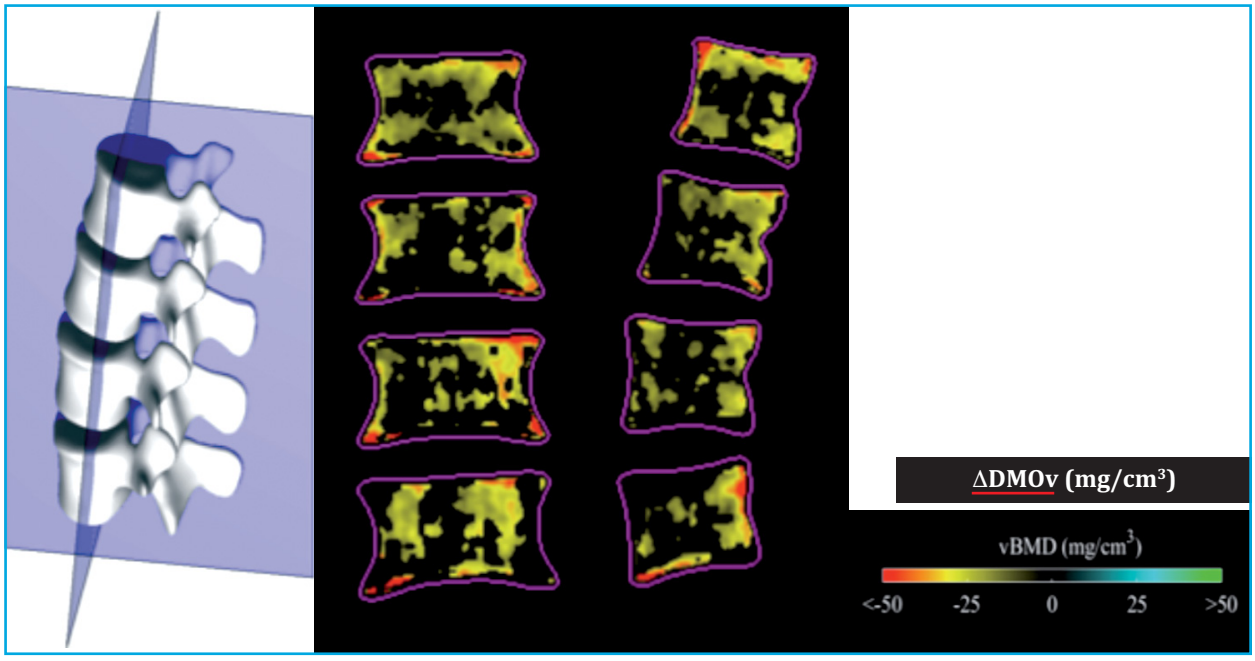

Figure 2. Map of the AUC calculated by using the trabecular vBMD in each voxel of the volumetric images of the subjects included in the experimental group and the control group. Only AUCs greater than the 90th percentile are represented (AUC >0.778). The maximum AUC registered is 0.930

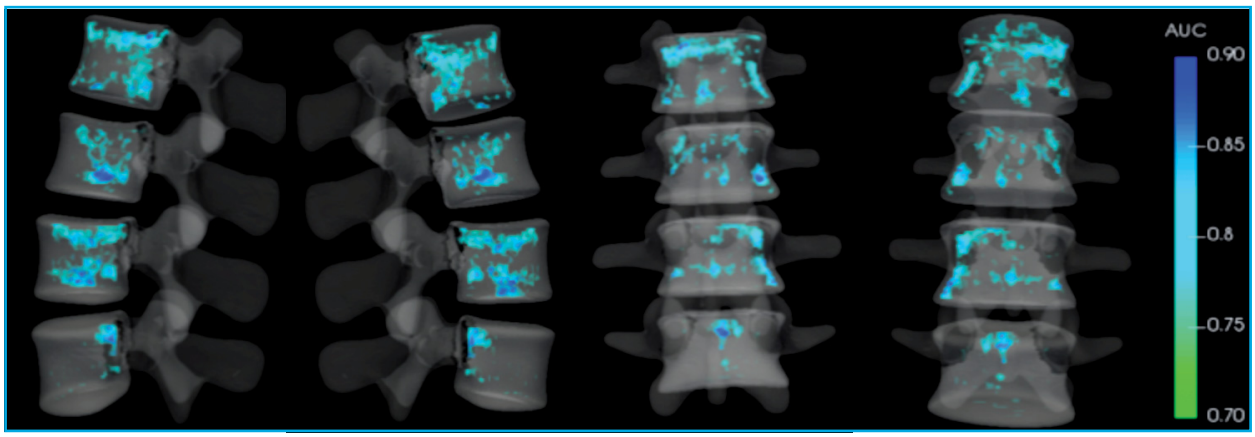

Figure 3. Top: anatomical distribution of the mean differences in the cortical sBMD of the vertebral body between the subjects included in the experimental group and the control group. Non-significant changes (unpaired Student t-test) are shown in grey. Bottom: AUC was calculated by using the cortical sBMD at each vertex of the vertebral body surface of the subjects included in the experimental group and the control group. The regions where the differences in the cortical sBMD were not significant (unpaired Student t-test), in the region of interest of the total vertebra, are shown in grey. The regions listed at an AUC greater than the 90th percentile (that is, an AUC>0.777) are circled in red. The maximum AUC was 0.836

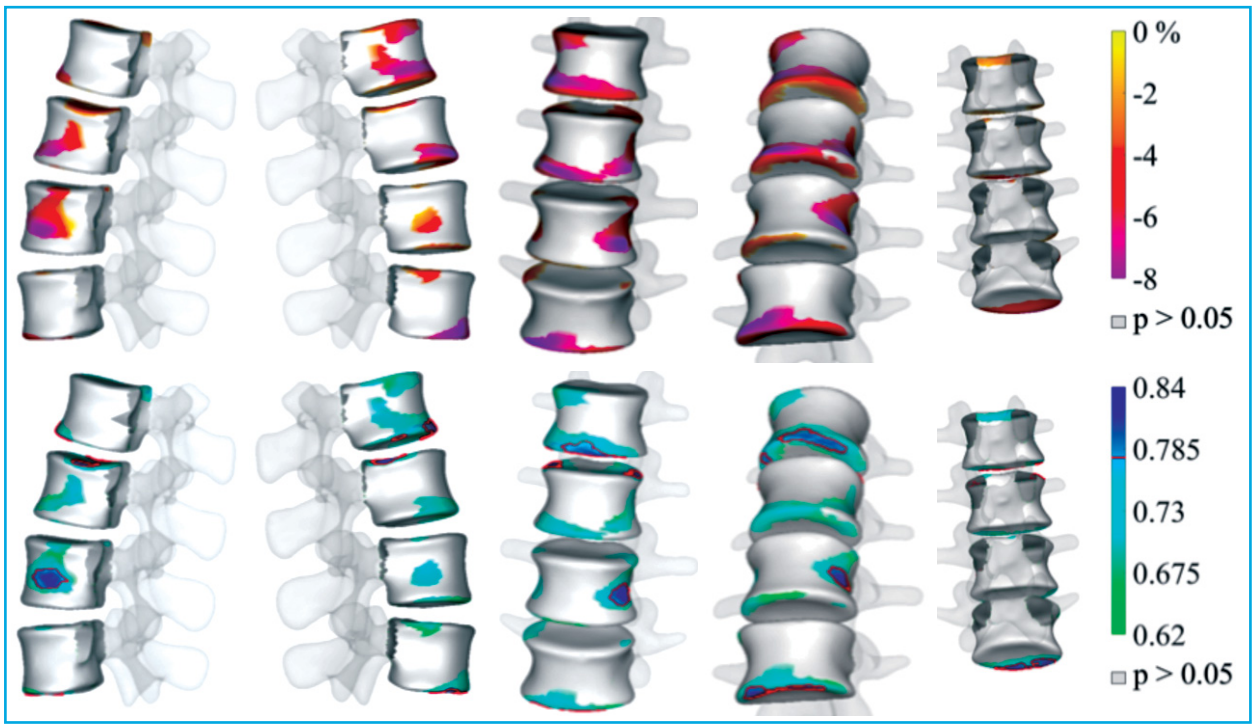

bral body (OR=4.557; 95% CI: 1.411-14.718 in the integral bone, and OR=5.060; 95% CI: 1.406-18.208 in the trabecular bone) in comparison with the aBMD (OR=1.862; 95% CI: 0.862-4.022). These results are consistent with various studies present in the literature, where it was found that the OR for QCT-derived measurements of vBMD are similar or higher, if compared with aBMD measurements[14,16]. Melton et al.[14] reported a slightly higher OR for vBMD in the L1-L3 segment (OR=2.2; 95% CI: 1.1-4.3) in the integral bone and OR=1.9; 95% CI: 1.0-3.6 in the trabecular bone), compared to aBMD (OR=0.7; 95% CI: 0.4-1.2). Anderson et al.[15] reported a higher OR for vBMD in L3 (OR=5.3; 95% CI: 1.3-21 in the integral bone and OR=5.6; 95% CI: 1.3-23.4 in the trabecular bone), compared to aBMD (OR=2.8; 95% CI: 1.0-8.0). Grampp et al.[16] reported a higher OR for vBMD in the L1-L4 segment (OR=3.0; 95% CI: 1.5-6.1 in the integral bone and OR=4.3; 95% CI: 1.8-10.1 in the trabecular bone), compared to aBMD (OR=2.4; 95% CI: 1.4-4.2).

The trabecular vBMD in the vertebral body was the measure that best discriminated between the experimental and the control groups, with an AUC of 0.801, compared to 0.662 for aBMD. Similar findings have been found in the literature in studies based on QCT[3,4,11-17,30]. Chalhoub et al.[13] reported an AUC of 0.79 for trabecular vBMD, compared to 0.72 for aBMD. Melton et al.[14] reported an AUC of 0.78 for trabecular vBMD, compared to 0.75 for aBMD. Grampp et al.[16] reported an AUC of 0.82 for trabecular vBMD, compared to 0.78 for aBMD. Imai et al.[20] reported an AUC of 0.77 for trabecular vBMD, compared to 0.71 for aBMD.

Degenerative diseases of the vertebral spine, abdominal aortic calcification, and other sclerotic lesions artificially increase the aBMD measure obtained in the AP DXA[3,4,11,30], despite the fact that patients with such pathologies have a higher risk of fracture. Trabecular vBMD in the vertebral body may be less sensitive to artifacts produced by these diseases, which are often found on the vertebral surface (cortical bone) or in the posterior arch. This could explain the higher AUC values found for the trabecular vBMD in our study. In this sense, 3D measurements derived from the DXA of the trabecular bone in the vertebral body could provide an alternative measure, overcoming the limitation of the diagnosis based on the aBMD by ruling out bone spurs, local deformations in the periosteal surface or in the posterior vertebral processes[30].

In the present study, the differences were less pronounced in the cortical bone (cortical sBMD: -10.1%, AUC=0.734) than in the trabecular bone (trabecular BMD: -16.2%, AUC=0.801). Biomedical studies demonstrated that the contribution of the cortical bone to the vertebral force is usually low in normal subjects, but it could be considerable in subjects with osteoporosis[30,31]. The precision of measurements derived from the DXA in the trabecular and the cortical bones was evaluated in previous works[27]. However, the cortex of the vertebral body is very thin (from 180 to 600 μm with an average thickness of 380 μm)[32], and DXA-based 3D modelling methods can hardly model local deformities, which could affect the precision of the cortical. Cortical sBMD is considered a stronger measure of cortical bone than cortical vBMD, since generally it is easier to measure in low-resolution images[31,32].

Local differences between the experimental and the control groups were analyzed using color-coded images. The mean differences in the trabecular vBMD between the subjects included in the experimental groups and those in the control group and their respective AUC were greater near the end plates and smaller in the centre of the vertebral body. Experimental studies of vertebral fractures in specimens show how the end plates of the vertebral body are the regions where failure at a tissue level begins[33-36]. These findings are consistent with biomechanical studies that show that the maximum load fraction on the trabecular bone normally occurs near the end plates[20,35,36]. The anatomical distribution of mean differences in cortical sBMD between subjects included in the thoracic spine fracture subgroup and their respective subjects in the control subgroup shows more pronounced differences in the end plates[33-36]. The results are consistent with biomechanical studies showing the thickness and density of the end plate, and the density of the adjacent trabecular bone as good predictors of local stiffness and strength.

The most significant limitation of the present study is the small number of subjects included. The main difficulties in including subjects in the experimental group were to find patients with DXA images from before the incident fracture, since most patients go to the doctor's office after the fracture event, and to ensure that the subjects did not present prevalent osteoporotic fractures in any bone at the time of the initial baseline visit. Furthermore, our study is monocentric, only includes postmenopausal Caucasian females and not all of them have the same fractured vertebra. Therefore, the results can only be extrapolated to populations with similar characteristics. Besides, due to the design of our study (retrospective and case-control), we cannot directly imply a causal association between the reduction of 3D measurements derived from DXA and osteoporotic fracture. Another limitation is that the participants included in this study did not undergo a QCT examination. Therefore, we were unable to make a direct comparison between the results obtained using 3D measurements derived from DXA and measurements derived from QCT. Nor was a comparison made of 3D measures derived from DXA and other methods used in clinical practice to predict fracture risk (such as the Trabecular Bone Score –TBS– or the FRAX® tool). Furthermore, the presence/absence of vertebral fracture was confirmed by anteroposterior DXA scans and vertebral morphometry (VFA, Vertebral Fracture Assessment). It would have been interesting to include other imaging modalities such as QCT or X-ray to further assess vertebral fractures.

Conclusions

This case-control study showed the association between 3D measurements derived from lumbar DXA and incident osteoporotic fractures in the dorsal vertebrae. The individuals in the experimental group showed lower values of vBMD measured in different vertebral regions and compartments compared to the values measured in the group of control subjects. Trabecular vBMD in the vertebral body was the measure that best discriminated between the experimental and control groups. Methods based on 3D modelling based on DXA could be a valuable option to complement standard 2D measurements derived from DXA in the management of osteoporosis. Similar studies involving larger cohorts will be conducted in future researches to determine whether 3D measurements derived from lumbar DXA could improve the prediction of fracture risk in clinical practice. Case-control studies will also be carried out with subjects presenting exclusively osteopenia according to the aBMD criteria.

Acknowledgments: We would like to thank the support of the Industrial Doctorate program of the Generalitat de Catalunya, as well as the QUAES Foundation - UPF Chair in Computational Tools for Health Purposes. The research that led to these results also received funding from the State Program for Research, Development and Innovation Oriented to the Challenges of Society, Ministry of Economy and Competitiveness (Reference: RTC-2014-2740-1) and from the Eurostars program (project ID: 9 140), financed by the Centre for Industrial and Technological Development, Ministry of Economy and Competitiveness. Furthermore, the author Mirella López Picazo received a FEIOMM grant to present the results of this work at the ASBMR 2018.

Conflict of interests: López Picazo M is an employee of Galgo Medical. Humbert L is a shareholder and employee of Galgo Medical. Di Gregorio S, González Ballester MA and Del Río Barquero LM have no conflicts of interest.

Bibliography

1. Johnell O, Kanis JA. An estimate of the worldwide prevalence and disability associated with osteoporotic fractures. Osteoporos Int. 2006;17:1726-33.
2. Ballane G, Cauley JA, Luckey MM, El-Hajj Fuleihan G. Worldwide prevalence and incidence of osteoporotic vertebral fractures. Osteoporos Int. 2017;28:1531-42.
3. Kanis JA. Diagnosis of osteoporosis and assessment of fracture risk. Lancet. 2002;359:1929-36.
4. Kanis J A, Johansson H, Oden A, McCloskey EV. Assessment of fracture risk. Eur J Radiol. 2009;71:392-7.
5. Marshall D, Wedel H. Meta-analysis of how well measures of bone mineral density predict occurrence of osteoporotic fractures. BMJ. 1996;312:1254-59.
6. Siris ES, Chen YT, Abbott TA, Barrett-Connor E, Miller PD, Wehren LE, et al. Bone mineral density thresholds for pharmacological intervention to prevent fractures. Arch Intern Med. 2004; 164:1108-12.
7. Dimai HP. Use of dual-energy X-ray absorptiometry (DXA) for diagnosis and fracture risk assessment; WHO-criteria, T- and Z-score, and reference databases. Bone. 2017;104:39-43.
8. Gordon CM, Lang TF, Augat P, Genant HK. Image-based assessment of spinal trabecular bone structure from high-resolution CT images. Osteoporos Int. 1998:8:317-25.
9. Genant HK, Wu CY, van Kuijk C, Nevitt MC. Vertebral fracture assessment using a semiquantitative technique. J Bone Miner Res. 1993;8:1137-48.
10. Prevrhal S, Fox JC, Shepherd JA, Genant HK. Accuracy of CT-based thickness measurement of thin structures: Modeling of limited spatial resolution in all three dimensions. Med Phys. 2003;30:1-8.
11. Li N, Li XM, Xu L, Sun WJ, Cheng XG, Tian W. Comparison of QCT and DXA: Osteoporosis detection rates in postmenopausal women. Int J Endocrinol. 2013;2013:895474.
12. Engelke K, Libanati C, Fuerst T, Zysset P, Genant HK. Advanced CT based in vivo methods for the assessment of bone density, structure, and strength. Curr Osteoporos Rep. 2013;11:246-55.
13. Chalhoub D, Orwoll ES, Cawthon PM, Ensrud KE, Boudreau R, Greenspan S, et al. Areal and volumetric bone mineral density and risk of multiple types of fracture in older men. Bone. 2016; 92:100-6.
14. Melton LJ 3rd, Riggs BL, Keaveny TM, Achenbach SJ, Hoffmann PF, Camp JJ, et al. Structural determinants of vertebral fracture risk. J Bone Miner Res. 2007;22:1885-92.
15. Anderson DE, Demissie S, Allaire BT, Bruno AG, Kopperdahl DL, Keaveny TM, et al. The associations between QCT-based vertebral bone measurements and prevalent vertebral fractures depend on the spinal locations of both bone measurement and fracture. Osteoporos Int. 2014;25:559-66.
16. Grampp S, Genant HK, Mathur A, Lang P, Jergas M, Takada M, et al. Comparisons of noninvasive bone mineral measurements in assessing age- related loss, fracture discrimination, and diagnostic classification. J Bone Miner Res. 1997;12:697-711.
17. Kopperdahl DL, Aspelund T, Hoffmann PF, Sigurdsson S, Siggeirsdottir K, Harris TB, et al. Assessment of incident spine and hip fractures in women and men using finite element analysis of CT scans. J Bone Miner Res. 2014;29:570-80.
18. Wang X, Sanyal A, Cawthon PM, Palermo L, Jekir M, Christensen J, et al. Prediction of new clinical vertebral fractures in elderly men using finite element analysis of CT scans. J Bone Miner Res. 2012;27:808-16.
19. Zysset P, Qin L, Lang T, Khosla S, Leslie WD, Shepherd JA, et al. Clinical use of quantitative computed tomography–based finite element analysis of the hip and spine in the management of osteoporosis in adults: the 2015 ISCD Official Positions-Part II. J Clin Densitom. 2015;18:359-92.
20. Imai K, Ohnishi I, Matsumoto T, Yamamoto S, Nakamura K. Assessment of vertebral fracture risk and therapeutic effects of alendronate in postmenopausal women using a quantitative computed tomography-based nonlinear finite element method. Osteoporos Int. 2009;20:801-10.
21. Ahmad O, Ramamurthi K, Wilson KE, Engelke K, Prince RL, Taylor RH. Volumetric DXA (VXA): A new method to extract 3D information from multiple in vivo DXA images. J Bone Miner Res. 2010;25:2744-51.
22. Väänänen SP, Grassi L, Flivik G, Jurvelin JS, Isaksson H. Generation of 3D shape, density, cortical thickness and finite element mesh of proximal femur from a DXA image. Med Image Anal. 2015;24:125-34.
23. Humbert L, Martelli Y, Fonolla R, Steghofer M, Di Gregorio S, Malouf J, et al. 3D-DXA: assessing the femoral shape, the trabecular macrostructure and the cortex in 3D from DXA images. IEEE Trans Med Imaging. 2017;36:27-39.
24. Whitmarsh T, Humbert L, Del Río Barquero LM, Di Gregorio S, Frangi AF. 3D reconstruction of the lumbar vertebrae from anteroposterior and lateral dual-energy X-ray absorptiometry. Med Image Anal. 2013;17:475-87.
25. López Picazo M, Magallon Baro A, Del Rio Barquero LM, Di Gregorio S, Martelli Y, Romera J, et al. 3D subject-specific shape and density estimation of the lumbar spine from a single anteroposterior DXA image including assessment of cortical and trabecular bone. IEEE Trans Med Imaging. 2018;37:1-12.
26. Van der Klift M, De Laet CE, McCloskey EV, Hofman A, Pols HA. The incidence of vertebral fractures in men and women: the Rotterdam Study. J Bone Miner Res. 2002;17:1051-6.
27. Budoff MJ, Hamirani YS, Gao YL, Ismaeel H, Flores FR, Child J, et al. Measurement of thoracic bone mineral density with quantitative CT. Radiology. 2010;257:434-40.
28. López Picazo M, Humbert L, Di Gregorio S, González Ballester MA, del Río Barquero LM. Discrimination of osteoporosis-related vertebral fractures by DXA-derived 3D measurements: a retrospective case-control study. Osteoporos Int. 2019;30:1099-110.
29. Humbert L, Hazrati Marangalou J, Del Río Barquero LM, van Lenthe GH, van Rietbergen B. Technical Note: Cortical thickness and density estimation from clinical CT using a prior thickness-density relationship. Med Phys. 2016; 43:1945-54.
30. Guglielmi G, Floriani I, Torri V, Li J, van Kuijk C, Genant HK, et al. Effect of spinal degenerative changes on volumetric bone mineral density of the central skeleton as measured by quantitative computed tomography. Acta Radiol. 2005;46:269-75.
31. Treece GM, Gee AH. Independent measurement of femoral cortical thickness and cortical bone density using clinical CT. Med Image Anal. 2015;20:249-64.
32. Winzenrieth R, Humbert L, Di Gregorio S, Bonel E, García M, Del Rio L. Effects of osteoporosis drug treatments on cortical and trabecular bone in the femur using DXA-based 3D modeling. Osteoporos Int. 2018;29:2323-33.
33. Noshchenko A, Plaseied A, Patel VV, Burger E, Baldini T, Yun L. Correlation of vertebral strength topography with 3-dimensional computed tomographic structure. Spine (Phila Pa 1976). 2013; 38(4):339-49.
34. Jackman TM, Hussein AI, Adams AM, Makhnejia KK, Morgan EF. Endplate deflection is a defining feature of vertebral fracture and is associated with properties of the underlying trabecular bone. J Orthop Res. 2014;32:880-6.
35. Eswaran SK, Gupta A, Adams MF, Keaveny TM. Cortical and trabecular load sharing in the human vertebral body. J Bone Miner Res. 2006;21:307-14.
36. Jackman TM, Hussein AI, Curtiss C, Fein PM, Camp A, De Barros L, et al. Quantitative, 3D visualization of the initiation and progression of vertebral fractures under compression and anterior flexion. J Bone Miner Metab. 2016;31:777-88.